Science of Tsunami Hazards **Volume 19, pages 150-159 (2001)**

A NON-LINEAR NUMERICAL MODEL FOR STRATIFIED TSUNAMI WAVES AND ITS APPLICATION

Monzur Alam Imteaz
Department of Civil Engineering
The University of Queensland
Brisbane, QLD 4072, Australia

Fumihiko Imamura
Disaster Control Research Centre
Tohoku University
Aoba, Sendai 980-8579, Japan

ABSTRACT

A non-linear numerical model is developed for the computation of water level and discharge for the propagation of a unidirectional two-layered tsunami wave. Four governing equations, two for each layer, are derived from Euler's equations of motion and continuity, assuming a long wave approximation, negligible friction and no interfacial mixing. A numerical model is developed using a staggered Leap-Frog scheme. The developed non-linear model is compared with an existing validated linear model developed earlier by the author for different non-dimensional wave amplitudes. The significance of non-linear terms is discussed. It is found that for simulations of the interface wave amplitude, the effect of non-linear terms is not significant. However, for the simulation of the top surface, the effect of non-linear terms is significant for higher wave amplitudes, and insignificant for lower wave amplitudes. Developed non-linear numerical model is used for the case of a progressive internal wave in an inclined bay. It is found that the effect of an adverse bottom slipe towards the direction of wave propagation is to amplify the wave. This amplification depends on the steepness of slope as well as the ratio of densities of upper layer fluid to lower layer fluid (α). Amplification increases with slope. For higher values of α, amplification of the top and interface surface decreases, which is reasonable. It is also found that even for a 4 percent density difference between upper layer and lower layer, amplification of the top surface will be twenty times higher than amplification in the non-stratified case. The model can be applied confidently to simulate the basic features of different practical problems, similar to those investigated in this study.

Science of Tsunami Hazards **Volume 19, pages 150-159 (2001)**

INTRODUCTION

Tsunamis are generated due to disturbances of free surface caused not only by seismic fault motion, but also by landslides and volcanic eruptions (Imamura and Imteaz, 1995). Tsunamis are categorized as a long wave and as such, long wave theory has been applied for the governing equations of tsunami propagation considering a single layer (i.e. equal density throughout the depth). But even with respect to the density gradient in deep sea, it is necessary to consider the stratified layers. An exchange between fresh water and saline water is known to limit the amount of mixing that can occur at the mouth of an estuary. In the case of landslide generated flows it is imperative to consider the mudflow as stratified. Two-layered long waves or flows in cases where underwater landslides have generating tsunamis has been studied by Hampton (1972), Parker (1982) and Harbitz (1991).

Analytical and experimental studies generally involve the flow of current over a horizontal bottom, which neglects the change in terrain over which atmospheric currents move and the change in height associated with avalanches. Studies on two-layered flow which consider current flowing over a non-horizontal bottom has been investigated by Benjamin (1968), Britter & Linden (1980) and Lin Po-Ching (1990). However, the use of small-scale physical model to design large structures may not reproduce the relative effects of viscosity, Reynolds number and some of the other design parameters.

Simulating the behaviour of two-layered flow has also been attempted numerically, however, for simplicity non-linear terms are often ignored. Some examples of linear numerical model can be found in Akiyama et al. (1990), Kranenburg (1993) and Imamura & Imteaz (1995). But accurate results can not be expected until simulations account for non-linear terms.

Jiang & Leblond (1992) developed a numerical model coupling a submarine landslide and the surface waves it generated. They have assumed the landslide as laminar flow of an incompressible viscous fluid and the water motion as irrotational. Long wave approximations were adopted for both water waves and mudslides. They have shown that three main waves are generated by a landslide. The first wave is a crest which propagates away from the mudslide site into deeper water. This crest is followed by a trough in the form of a forced wave which propagates with the speed of the mudslide front and the third wave is a relatively small trough which propagates shoreward. They have also found that two major parameters dominate the interaction between the slide and waves it produces: the density of sliding material and the depth of water at the mudslide site. The findings are similar to those of Imamura & Imteaz (1995).

Considering non-linear terms an adequate numerical model for simulating two-layer flow on non-horizontal bottom is attempted. Moreover, the model was extended to actual or field condition.

NOTATIONS

ρ = Density of fluid
M = Discharge per unit width of flow
η = Water surface elevation above still water level
α = Density ratio of upper layer fluid to lower layer fluid
h = Still water depth
x = Distance in downstream direction
t = Axis representing time

g = Acceleration due to gravity
i = Spatial node points in a finite difference scheme
n = Temporal node points in a finite difference scheme
β = Depths ratio of lower layer to upper layer
k = Wave number
L = Wave length
a = wave amplitude

THEORETICAL BACKGROUND

A mathematical model for two-layer flow in a wide channel with non-horizontal bottom was set up assuming a hydrostatic pressure distribution, negligible friction and negligible interfacial mixing. Also uniform density and velocity distributions in each layer was assumed. Considering a two dimensional case as shown in Figure 1, using Euler's equation of motion and continuity for each layer, by integrating the equations for specified limit of each layer and applying long wave approximation (i.e. vertical accelerations are negligible) and boundary conditions, following integrated governing equations were derived. The derivations are explained in details by Imteaz, M.A. (1994).

For upper layer-
Mass conservation equation,

$$\frac{\partial M_1}{\partial x} + \frac{\partial(\eta_1 - \eta_2)}{\partial t} = 0 \qquad (1)$$

and momentum equation,

$$\frac{\partial M_1}{\partial t} + \frac{\partial(M_1^2 / D_1)}{\partial x} + g D_1 \frac{\partial \eta_1}{\partial x} = 0 \qquad (2)$$

For lower layer-

Mass conservation equation, $\frac{\partial M_2}{\partial x} + \frac{\partial \eta_2}{\partial t} = 0$ (3)

and momentum equation,

$$\frac{\partial M_2}{\partial t} + \frac{\partial(M_2^2 / D_2)}{\partial x} + g D_2 \left\{ \alpha \left(\frac{\partial \eta_1}{\partial x} + \frac{\partial h_1}{\partial x} - \frac{\partial \eta_2}{\partial x} \right) + \frac{\partial \eta_2}{\partial x} - \frac{\partial h_1}{\partial x} \right\} = 0 \qquad (4)$$

Where,
η_1 = Water surface elevation above still water level of layer '1'
η_2 = Water surface elevation above still water level of layer '2'
$D_1 = \eta_1 + h_1 - \eta_2$
$D_2 = h_2 + \eta_2$
h_1 = Still water depth of layer '1'
h_2 = Still water depth of layer '2'
$\alpha = \rho_1/\rho_2$

$$M_1 = \int_{-h_1+\eta_2}^{\eta_1} u_1 dy, M_2 = \int_{-h_1-h_2}^{-h_1+\eta_2} u_2 dy$$

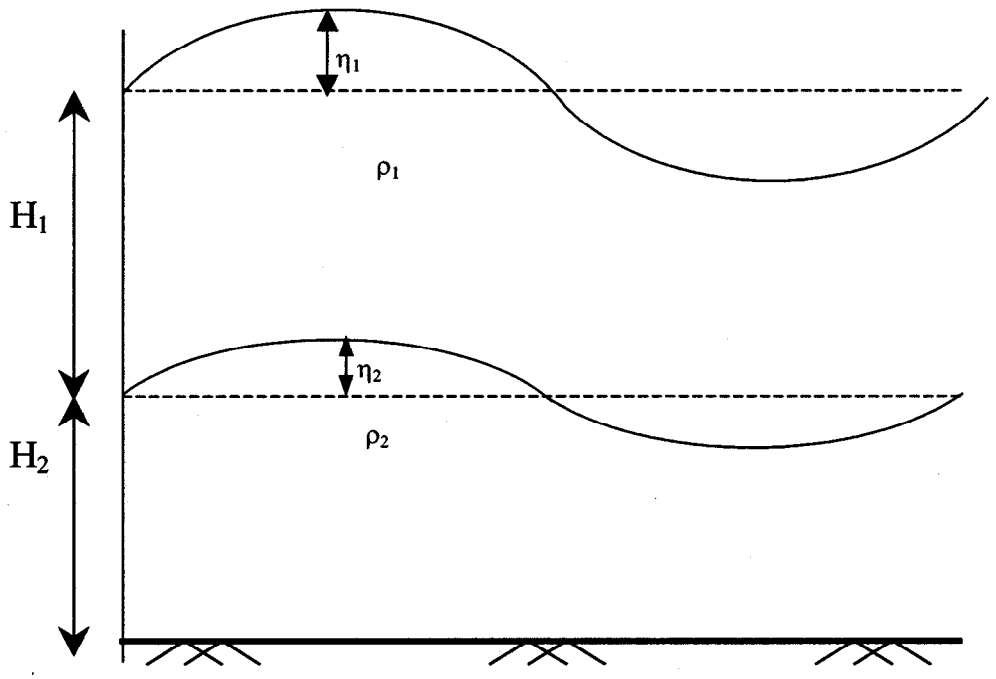

Figure 1 Schematic diagram of a two-layer profile

NUMERICAL MODEL

It is very difficult to solve the governing non-linear equations analytically, however, a finite difference scheme using a staggered leap-frog scheme can provide a numerical solution. This scheme has been used previously for the solution of linearized governing equations with good results (Imamura & Imteaz, 1995). This scheme is one of the explicit central difference scheme with the truncation error of second order. The staggered scheme considers that the computation points for the water surface elevation (η) does not coincides with the computation points for discharge (M). There are half step differences (½Δt for temporal and ½Δx for spatial) between computation points of two variables, η and M (as shown in Figure 2). Finite difference equations for this scheme are as follows.

Mass conservation equation for the upper layer,

$$\frac{\eta_{1,i}^{n+1/2} - \eta_{1,i}^{n-1/2} - \eta_{2,i}^{n+1/2} + \eta_{2,i}^{n-1/2}}{\Delta t} + \frac{M_{1,i+1/2}^{n} - M_{1,i-1/2}^{n}}{\Delta x} = 0 \qquad (5)$$

Mass conservation equation for the lower layer,

$$\frac{\eta_{2,i}^{n+1/2} - \eta_{2,i}^{n-1/2}}{\Delta t} + \frac{M_{2,i+1/2}^{n} - M_{2,i-1/2}^{n}}{\Delta x} = 0 \qquad (6)$$

Momentum equation for the upper layer,

$$\frac{M_{1,i+1/2}^{n} - M_{1,i+1/2}^{n-1}}{\Delta t} + g\frac{D_{1,i+1}^{n-1/2} + D_{1,i}^{n-1/2}}{2}\frac{\eta_{1,i+1}^{n-1/2} - \eta_{1,i}^{n-1/2}}{\Delta x} +$$

$$\frac{(M_{1,i+1/2}^{n-1})^2}{(D_{1,i+1}^{n-1/2}+D_{1,i}^{n-1/2}+D_{1,i+1}^{n-3/2}+D_{1,i}^{n-3/2})/4}-\frac{(M_{1,i-1/2}^{n-1})^2}{(D_{1,i}^{n-1/2}+D_{1,i-1}^{n-1/2}+D_{1,i}^{n-3/2}+D_{1,i-1}^{n-3/2})/4}=0 \quad (7)$$

Momentum equation for the lower layer,

$$\frac{M_{2,i+1/2}^{n}-M_{2,i+1/2}^{n-1}}{\Delta t}+g\frac{(D_{2,i+1}^{n-1/2}+D_{2,i}^{n-1/2})}{2}$$

$$\frac{\alpha(\eta_{1,i+1}^{n-1/2}-\eta_{1,i}^{n-1/2})+(\alpha-1)(h_{1,i+1}-h_{1,i})+(1-\alpha)(\eta_{2,i+1}^{n-1/2}-\eta_{2,i}^{n-1/2})}{\Delta x}+$$

$$\frac{(M_{2,i+1/2}^{n-1})^2}{(D_{2,i+1}^{n-1/2}+D_{2,i}^{n-1/2}+D_{2,i+1}^{n-3/2}+D_{2,i}^{n-3/2})/4}-\frac{(M_{2,i-1/2}^{n-1})^2}{(D_{2,i}^{n-1/2}+D_{2,i-1}^{n-1/2}+D_{2,i}^{n-3/2}+D_{2,i-1}^{n-3/2})/4}=0 \quad (8)$$

Where 'n' denotes the temporal grid points and 'i' denotes the spatial grid points as shown in Figure 2. To calculate 'D' values at the computation point of 'M', the average of four surrounding 'D' values is required.

In the spatial direction all η_1, η_2 values at step 'n-1/2' and all M_1, M_2 values at step '(n-1)' are assigned as initial conditions. For all later time steps at left and right boundaries, values of M_1 and M_2 are calculated by a characteristic method, which uses the values of previous time steps and wave celerity. The finite difference momentum equations for the upper and lower layer allows M_1 and M_2 values at step 'n' to be calculated. Then using the latest values of M_2 and deduced finite difference continuity equation for lower layer all values of η_2 at step '(n+1/2)' can be calculated. Then using the latest values of η_2, M_1 and deduced finite difference continuity equation for upper layer, all values of η_1 at step '(n+1/2)' are calculated. Similarly using new values of η_1, η_2, M_1, M_2 as initial conditions, calculations can be proceeded in time direction up to desired step. As initial condition (i.e. at t = 0) all η_1 and M_1 values are taken as zero. For interface, initial condition was found by substituting t = 0 in the known expression of η_2, which gives,

$$\eta_2 = a_2 \mathrm{Sin}(kx) = a_2 \mathrm{Sin}(\frac{2\pi}{L}x)$$

A linear relationship between the water level and discharge is used to determine an expression for M_2 i.e.,

$$M_2 = \sqrt{(g/H_2)}\,\eta_2(H_2+\eta_2)$$

COMPARISON WITH LINEAR MODEL

Simulations of the numerical model were performed for different values of initial interface wave amplitude, a_2. For these simulations, α=0.2, β=1.0, ΔX=10 m, ΔT=0.2 sec, h_1=25 m, h_2=25 m have been chosen and kept constant for different simulations. Simulations were performed separately for a_2= 2 m, 6 m and 8 m with periods of 4 sec, 6 sec and 8 sec. Results were compared with known linear model results using the same input parameters. Results are shown graphically in Figures 3, 4 and 5 for a_2 = 2 m, 6 m and 8 m respectively. From the figures it is seen that for a_2 = 2 m (a_2/h_2=0.08) linear and non-linear model results are almost identical. This indicates the insignificance of non-linear terms and confirms that for $\eta/h < 0.1$, the effect of non-linear terms is negligible.

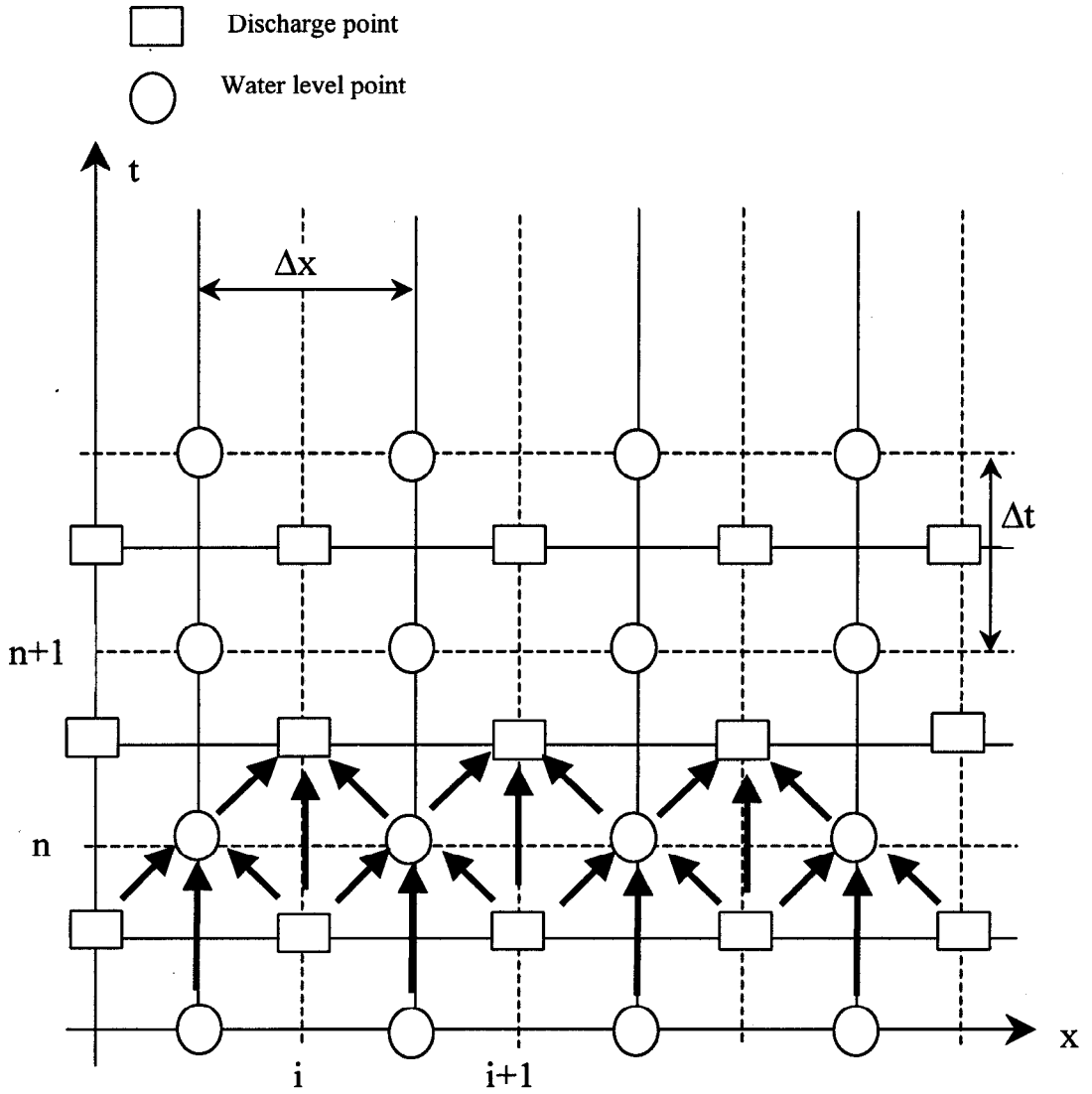

Figure 2 Schematic diagram of the staggered leap-frog scheme

For simulations with a_2 = 6 m and 8 m, it is found that there is a significant difference between linear and non-linear model, proving that for $\eta/h > 0.1$ non-linear terms are significant. For the modelled interface differences arise as a result of the wave celerity. Due to inclusion of η in the wave celerity, $\sqrt{\{g(h+\eta)\}}$, non-linear wave celerity is greater than the linear wave celerity. For this reason it is seen that non-linear waves propagate with greater speed and become steeper as time progresses. The above mentioned reasoning also accounts for the marked difference between linear and non-linear top surface levels, η_1. It is observed that this difference increases with the value of interface amplitude, a_2. For higher values of a_2, values of η_1 will increase. As can be seen any increase a_2 of values will cause increase of η_1 values, (i.e increase of η_1/h_2 values) and for higher η_1/h_2 non-linear terms become more significant.

APPLICATION OF THE MODEL

A progressive internal wave into an inclined bay, which is related with a sudden exchange of water in the bay was considered as an application for the numerical model. This condition may occur due

to an internal tide wave into the bay. For this condition a sloping bottom is assumed with a vertical wall at the downstream end. As an upstream boundary condition, the interface water surface is assumed to be known and a function of time. A downstream boundary condition involves setting the discharge of both layers, M_1 and M_2 as zero.

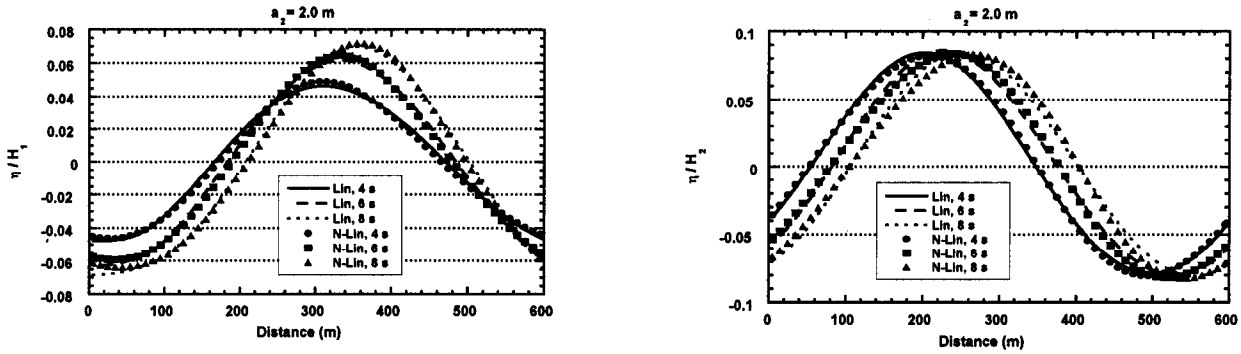

(a) (b)

Figure 3 Comparison of linear and non-linear model for (a) top surface and (b) interface (a_2=2 m)

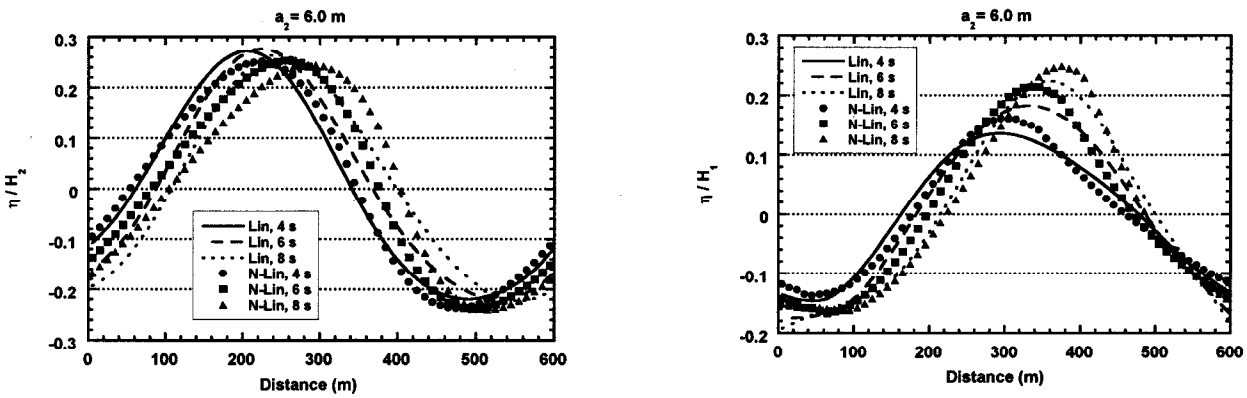

(a) (b)

Figure 4 Comparison of linear and non-linear model for (a) top surface and (b) interface (a_2=6 m)

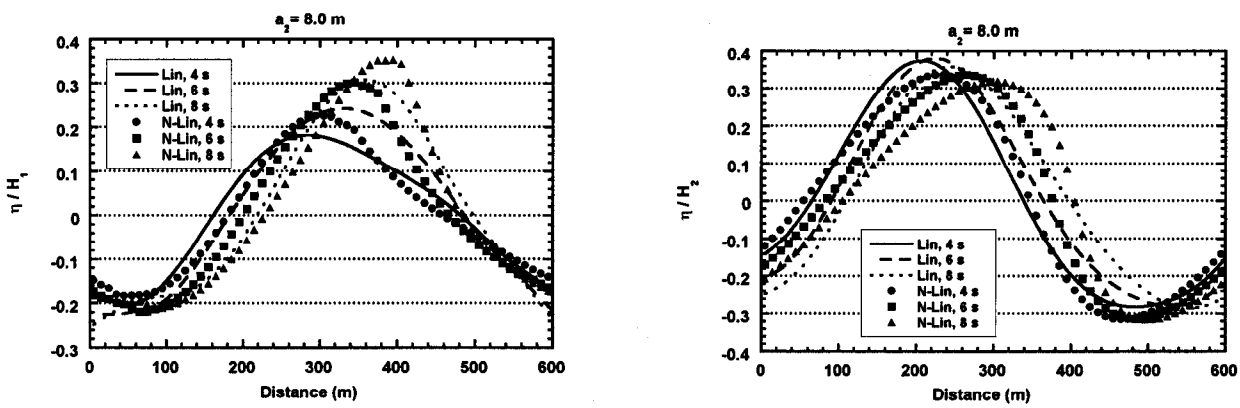

(a) (b)

Figure 5 Comparison of linear and non-linear model for (a) top surface and (b) interface (a_2=8 m)

In general it was found that a sloping bottom amplifies wave as it propagates. So for longer travel distance amplification will be higher. Simulations were performed for different slopes and different 'α' values. To show the effect of 'α', model results for α = 0.1, 0.4, keeping other parameters constant have shown in Figure 6(a) and 6(b). In these cases slope was assumed as 0.1, computational length 200 m, u/s h_2= 25 m, at d/s h_2= 5 m and h_1= 10 m (constant). From these figures it is clear that when 'α' increases the amplification of top surface decreases and vice versa. For interface amplification decreases as 'α' increases, which is opposite as discussed by Imamura & Imteaz (1995) for the case of free transmission (no vertical wall at d/s end). This is due to presence of vertical wall and rigorous interaction at d/s end by the reflected upper layer wave. To see the effect of stratification, model was again simulated for α=1.0 (i.e. same density for both the layers) keeping other conditions same as in Figure 6(a) and 6(b). From Figure 7(a) it is found that amplification of top surface is very low for this case, which is not real, as in reality there is always some stratification. Figure 8 shows the ratio of top surface amplitudes of stratified case to non-stratified case for several density difference in percent. It is shown that even for a 4% density difference between upper layer and lower layer, amplification of top surface will be twenty times higher than the amplification in non-stratified case. This warns serious error in calculation if uniform water density is considered for the case of Tsunami and long waves.

To show the effect of slope change on amplification, simulation was carried out for two different slopes, keeping other parameters (ΔX, ΔT, α, u/s and d/s h_1, u/s h_2) constant. At d/s h_2 can not be constant to allow the variation of slope and to keep the h_2 at u/s, computational length constant. Computational length should be keep constant, the amplification at the d/s end is the cumulative effect of slope used, so change in computational length will affect the result. For the same α Figure 6(a) shows the amplification of top surface for slope equals to 0.1 and Figure 7(b) shows for slope equals to 0.075. It is found from these figures that as slope decreases amplification of both top surface and interface also decreases which is reasonable. Presented results are not indicating the sole effect of slope variation, because there is a change of depth 'h_2' at right side boundary. At right side 'h_2' has to increase to provide decreasing slope in computation. But 'h_2/h_1' ratio also affects the amplification of top surface. In the above-mentioned cases, change of h_2/h_1 at right side boundary causes opposite the effect of slope changes.

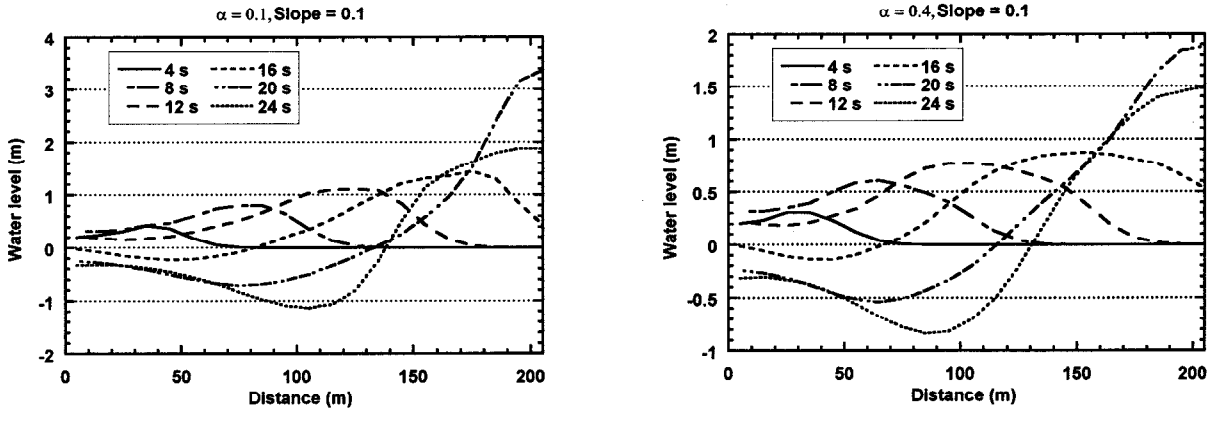

(a) (b)

Figure 6 Amplification of the top surface for (a) α= 0.1 and (b) α=0.4 having slope=0.1

CONCLUSION

A numerical model using a staggered leap-frog scheme has been used to ascertain the effect of including non-linear terms in the governing equations of two-layered flow. Comparison has been

made against the linear model of Imteaz, M.A. (1994). Non-linear terms were found to be insignificant for low (< 0.1) η/h_2 ratio, however non-linear terms are highly significant for higher η/h_2 ratio. Therefore in the cases of high η/h_2 ratio and where amplitude amplifies due to slope or vertical wall, non-linear model should be used to simulate the actual condition.

The developed model was applied to the case of rapid exchange of water in the bay, considering non-horizontal bottom, two-layer flow and vertical wall at the shore. In this case constant bottom slope and horizontal interface was assumed, but model can handle for cases of any arbitrary bottom and any arbitrary interface as well as top surface. Effects of sloping bottom and relative density of two layers were investigated. It was found that, presence of adverse slope to the direction of wave propagation causes to amplify the propagating wave as wave propagates, which is reasonable. Again it was found that as 'α' increases amplification of top surface decreases and vice versa, which is reasonable. It must also be noted that the phenomena of shoaling for a single layer flow can not be used as a comparison for the investigated two layer flow.

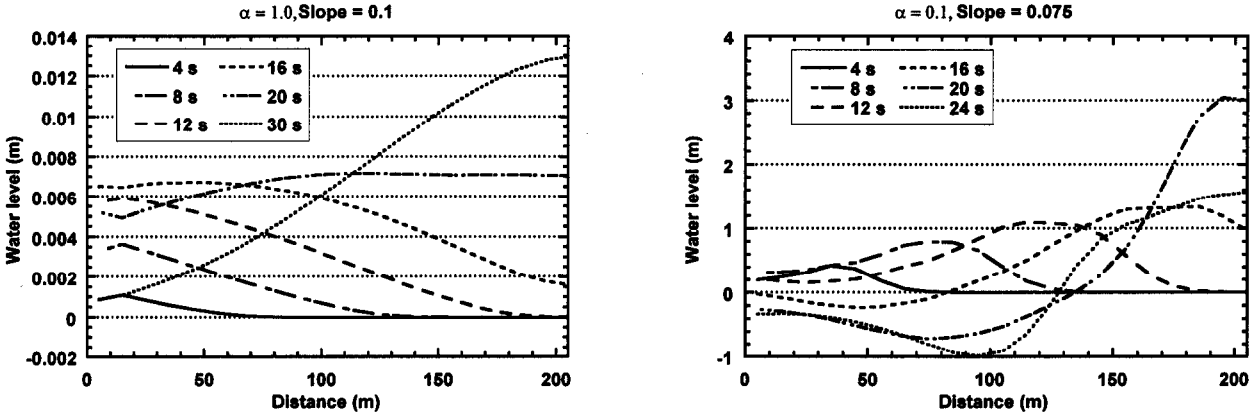

(a) (b)

Figure 7 Amplification of the top surface for (a) α= 1, slope=0.1 and (b) α= 0.1, slope=0.075

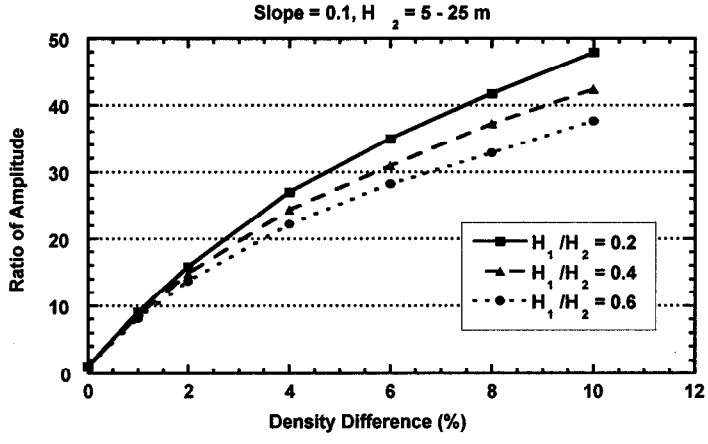

Figure 8 Ratio of top surface amplitudes for stratified case to non-stratified case

REFERENCES

AKIYAMA, J., WANG, W. AND URA, M. (1990) Numerical Model of Unsteady Gravity Currents, Proc. 7th Congress, APD, IAHR, Beijing.

BENJAMIN, T.B. (1968) Gravity Currents and Related Phenomena, J. Fluid Mech., Vol.31, pp.209-248.

BRITTER, R.E. AND LINDEN, P.F. (1980) The Motion of the Front of a Gravity Current Travelling Down an Incline, J. Fluid Mech., Vol.99, pp.531-543.

HAMPTON, M.H. (1972) The Role of Subaqueous Debris Flow in Generating Turbidity Currents, J. Sedimentary Petrology, Vol. 42, No. 4, pp.775-793.

HARBITZ, C. (1991) Numerical Simulation of Slide Generated Water Waves, Sci. of Tsunami Hazards, Vol. 9, No. 1, pp. 15-23.

IMAMURA, F. AND IMTEAZ, M.A. (1995) Long Waves in Two Layers: Governing Equations and Numerical Model, Sc. of Tsunami Hazards, Vol. 13, No. 1, pp. 3-24.

IMTEAZ, M.A. (1994) Numerical Model for the Long Waves in Two Layers, AIT Thesis, No. WA-94-2.

JIANG, L. AND LEBLOND, P.H. (1992) The Coupling of a Submarine Slide and the Surface Waves which it Generates, J. of Geophys. Res., Vol. 97, No. C8, pp. 12713-12744.

KRANENBURG, C. (1993) Unsteady Gravity Currents Advancing along a Horizontal Surface, J. Hydraulic Research, Vol.31, pp.49-60.

LIN, PO-CHING (1990) Experiments on Discontinuous Gravity Currents over a Slope, AIT Thesis, No. WA-90-23.

PARKER, G. (1982) Conditions for Ignition of Catastrophically Erosive Turbidity Currents, Marine Geology, Vol. 46, pp. 307-327.